

Pooling strength amongst limited datasets using hierarchical Bayesian analysis, with application to pyroclastic density current mobility metrics

Sarah Ogburn^{1,2} James Berger³ Eliza Calder⁴
Danilo Lopes⁵ Abani Patra⁶ Bruce Pitman⁷
Regis Rutarindwa⁸ Elaine Spiller⁸ Robert L. Wolpert³

March 5, 2016

¹State University of New York, University at Buffalo, Department of Geology, Buffalo, NY 14260.

²*Now at:* U.S. Geological Survey and U.S. Agency for International Development, Volcano Disaster Assistance Program (VDAP), Vancouver, WA, 98683. sogburn@usgs.gov

³Duke University, Department of Statistical Sciences, Durham, NC 27708.

⁴University of Edinburgh, School of Geosciences, EH9 3FE, UK

⁵Federal University of Sao Carlos, Brazil

⁶State University of New York, University at Buffalo, Department of Aerospace and Mechanical Engineering, Buffalo, NY 14260.

⁷State University of New York, University at Buffalo, Department of Mathematics, Buffalo, NY 14260.

⁸Marquette University, Department of Mathematics, Statistics, and Computer Science, Milwaukee, WI 53201.

Abstract

In volcanology, the sparsity of datasets for individual volcanoes is an important problem, which, in many cases, compromises our ability to make robust judgments about future volcanic hazards. In this contribution we develop a method for using hierarchical Bayesian analysis of global datasets to combine information across different volcanoes and to thereby improve our knowledge at individual volcanoes. The method is applied to the assessment of mobility metrics for pyroclastic density currents in order to better constrain input parameters and their related uncertainties for forward modeling. Mitigation of risk associated with such flows depends upon accurate forecasting of possible inundation areas, often using empirical models that rely on mobility metrics measured from the deposits of past flows; or on the application of computational models, several of which take mobility metrics, either directly or indirectly, as input parameters. We use hierarchical Bayesian modeling to leverage the global record of mobility metrics from the FlowDat database, leading to considerable improvement in the assessment of flow mobility where the data for a particular volcano is sparse. We estimate the uncertainties involved and demonstrate how they are improved through this approach. The method has broad applicability across other areas of volcanology where relationships established from broader datasets can be used to better constrain more specific, sparser, datasets. Employing such methods allows us to use, rather than shy away from, limited datasets; and allows for transparency with regard to uncertainties, enabling more accountable decision-making.

25 **1 Introduction**

26 Efforts in quantitative volcanic hazards assessment (QVHA) are currently being
27 bolstered by a number of ongoing initiatives to compile important databases such
28 as the Global Volcanism Program database [Global Volcanism Program, 2013],
29 WOVOdat [Venezky and Newhall, 2007], Geologic Survey of Japan (GSJ) Qua-
30 ternary and Active volcanoes databases [Geological Survey of Japan and the Na-
31 tional Institute of Advanced Industrial Science and Technology (AIST), 2013],
32 LaMEVE [Crosweller et al., 2012], DomeHaz [Ogburn, 2012a, Ogburn et al.,
33 2015], and FlowDat [Ogburn, 2012b, 2014]. These efforts collectively reflect a
34 growing understanding of the value that is added by undertaking global analysis.
35 Challenges remain, however, in dealing with variable data quality, sparse data for
36 particular volcanic systems, and quantification of uncertainty. Some of these out-
37 standing issues can be dealt with by exploring and developing statistical methods,
38 which can not only improve our predictive capacity for future eruptions but can
39 also contribute to advancing our scientific understanding of the volcanic processes
40 involved.

41 Data sparsity, in particular, is a ubiquitous problem when assessing volcanic
42 hazards [Siebert et al., 2010]. Indeed, Siebert et al. [2010] posit that “poorly
43 known, thickly vegetated, long-quiescent volcanoes that have had no historical
44 activity...may be the most dangerous of all.” The record of activity at any given
45 volcano may be incomplete or heavily biased due to inadequate or differential
46 preservation and exposure of the deposits, or the history of nearby human set-

47 tlement [e.g. Crosweller et al., 2012, Brown et al., 2014, Kiyosugi et al., 2015,
48 Whelley et al., 2015]. Other practical issues, such as accessibility and remoteness
49 [e.g. Whelley et al., 2015], also hinder investigation and therefore influence data
50 completeness. In many cases, scientific interest in a given system is driven by
51 significant observable volcanic activity, while small magnitude or effusive activ-
52 ity often poorly recorded [Deligne et al., 2010, Furlan, 2010, Siebert et al., 2010,
53 Crosweller et al., 2012, Brown et al., 2014]. Often, newly active volcanoes, espe-
54 cially those that had previously been dormant [e.g. Chaitén, Chile, 2008; Alfano
55 et al., 2011, Watt et al., 2013], may be poorly understood and may simply lack
56 sufficient information on which to base assessments about renewed and future
57 behavior.

58 The issues discussed above often result in information concerning a particular
59 type of phenomenon (such as pyroclastic density currents) being plentiful at some
60 well-studied volcanoes but very limited at others. Two end-member approaches to
61 deal with this problem are: 1) to assume that particular phenomena have similar
62 characteristics at every volcano, and thus use information from the global record
63 of all volcanoes; or 2) to assume that particular phenomena at different volcanoes
64 behave dissimilarly, and thus use only the information from a given volcano. Of-
65 ten, however, it is reasonable to assume that a particular volcanic phenomenon,
66 while not identical across volcanoes, is controlled by similar processes, and can
67 be assumed to vary according to some probability distribution. This allows one
68 to “borrow” information from a global database, leading to better quantification
69 of uncertainty and improved accuracy in hazard assessment at a particular vol-

70 cano. The statistical methodology for doing this is hierarchical Bayesian analysis
71 [Allenby et al., 2005]. Bayesian approaches to volcanic hazard assessment have
72 been used successfully for event tree construction [Marzocchi et al., 2008, 2010]
73 and have recently been expanded using hierarchical Bayesian methods [Sheldrake,
74 2014].

75 In this work, we use hierarchical Bayesian methods to augment statistical anal-
76 ysis of the mobility of pyroclastic density currents. Specifically for this work, our
77 interest is in dense, concentrated dome-collapse pyroclastic density currents. Py-
78 roclastic density currents (PDCs) are hot avalanches of rock and gas which, due
79 to their ability to travel great distances at high speeds, are among the most de-
80 structive volcanic hazards. This effort, in part, is motivated by the need for more
81 robust characterization of the mobility relationships of PDCs for different vol-
82 canic systems. Mitigation of risk associated with these phenomena depends upon
83 accurate forecasting of possible flow paths and inundation areas, often using em-
84 pirical models that rely on mobility metrics (e.g. the energy cone model, Malin
85 and Sheridan [1982]; PFz, Widiwijayanti et al. [2008]) or the application of com-
86 putational flow models (e.g. TITAN2D Patra et al. [2005]; VolcFlow, Kelfoun and
87 Druitt [2005]). Linear regression of mobility metrics such as the Heim coefficient
88 (height dropped/runout length of a PDC, or H/L) or the relationship between the
89 area inundated by a PDC and its volume, often informs such models, sometimes as
90 direct model inputs (e.g., the energy cone model, PFz), or indirectly as proxies for
91 input parameters (e.g., basal friction angle in TITAN2D, constant resisting shear
92 stress in VolcFlow). There are many examples where such data has been used suc-

93 cessfully to simulate and replicate the behavior of past events [Kelfoun and Druitt,
94 2005, Widiwijayanti et al., 2008, Charbonnier and Gertisser, 2009, 2012, Murcia
95 et al., 2010, Sheridan et al., 2010, Capra et al., 2011, Ogburn, 2014]. However,
96 the use of such data as input parameters in forward modeling of future hazards is
97 compromised by the relative dearth of information on large volume events and the
98 scarcity of data from remote, under-studied, or recently active volcanoes. When
99 eruptive activity initiates at a newly active volcano, for which little PDC data
100 is available, forward modeling by simply substituting PDC mobility parameters
101 from other volcanoes is of tenuous merit, as local source conditions and topo-
102 graphic effects influence flow mobility [Stinton, 2014, Charbonnier and Gertisser,
103 2011, Lube et al., 2011, Ogburn, 2014] and inundation estimates will have high
104 uncertainties. Instead, what is required are more accountable approaches to en-
105 able the use of the limited existing data to their maximum potential while also
106 quantifying the associated uncertainty.

107 Here we develop a method using hierarchical Bayesian analysis to leverage the
108 global record of mobility metrics from the FlowDat mass flow database [Ogburn,
109 2012b, 2014]. We borrow strength from the global record to understand mobility
110 characteristics at specific volcanoes, leading to considerable improvement in as-
111 sessments where data for a particular volcano is sparse. We first present we first
112 present the background to the problem of assessing mobility of PDCs and how
113 PDC mobility metrics are used with, and subsequently propagated through, flow
114 modeling (section 2). The hierarchical Bayesian analysis of the compiled data
115 is presented in section 3, and the results discussed in section 4. The variables

116 and abbreviations used throughout are presented in Appendix A and step-by-step
117 details of the method are provided in Appendix B.

118 **2 Mobility metrics for mass flows**

119 **2.1 Frictional vs. resisting shear stress models**

120 The most widely used mobility metric for concentrated mass flows of (e.g. vol-
121 canic and non-volcanic debris avalanches, dome- and column-collapse PDCs) is
122 the Heim coefficient [Heim, 1932], commonly denoted as H/L , where H is the
123 vertical fall height traversed by a flow and L is the runout length. H/L is equiv-
124 alent to the coefficient of friction following a Mohr-Coulomb friction model, in
125 which shear stress at the initiation of failure is proportional to the normal stress.

126 According to Mohr-Coulomb friction models, the mass or volume, V , of the
127 flow should be irrelevant to mobility, and the coefficient of friction should be a
128 function of material properties. Numerous studies of real deposits, however, have
129 shown a linear inverse relationship between $\log(V)$ of a mass flow (of any type)
130 and $\log(H/L)$ [Heim, 1932, Scheller, 1971, Scheidegger, 1973, Hsü, 1975], with
131 large volume flows demonstrably being more mobile than small volume flows.

132 An alternative to the frictional model approach is that of the constant resisting
133 shear stress models. In these models, the mobility of mass flows is described by a
134 constant resisting shear stress (CRS), or yield strength, and planimetric area, A_p ,
135 is related to $V^{2/3}$ via scaling arguments [Hungr, 1990, Iverson et al., 1998, Dade
136 and Huppert, 1998, Calder et al., 1999]. This model indicates a relationship be-

137 tween inundated area and resisting shear stress, suggesting a yield stress rheology
138 [Kilburn and Sørensen, 1998, Crosta et al., 2003, Griswold and Iverson, 2008].

139 Both these metrics (H/L and A_p vs. $V^{2/3}$) have been applied to PDC mobility
140 with success [Sparks, 1976, Nairn and Self, 1978, Francis and Baker, 1977, Sheri-
141 dan, 1979, Begét and Limke, 1988, Fisher and Schmincke, 1984, Hayashi and
142 Self, 1992, Calder et al., 1999, Cole et al., 2002, Vallance et al., 2010, Charbon-
143 nier and Gertisser, 2011] and have become standard mobility metrics with which
144 to compare and contrast PDC behavior, especially, but not exclusively, those of
145 concentrated PDCs.

146 **2.2 Mobility metrics for flow modeling**

147 Many empirical flow inundation models are based directly on measurements of
148 H/L or A_p vs. $V^{2/3}$. Hsü [1975], Sheridan [1979], and Malin and Sheridan
149 [1982] first used the ‘energy-line’ or ‘energy-cone’ concept (which is defined by
150 H/L). This concept has been applied at a variety of volcanoes [e.g. Sheridan and
151 Malin, 1983, Wadge and Isaacs, 1988, Höskuldsson and Cantagrel, 1994, Alberico
152 et al., 2002, Sheridan et al., 2004] and also forms the basis for the FLOW2D and
153 FLOW3D computer models [e.g. Kover and Sheridan, 1993, Martin del Pozzo
154 et al., 1995, Sheridan and Macías, 1995, Hooper and Mattioli, 2001] which base
155 shear resistance on basal friction (taken directly from H/L), viscosity, and turbu-
156 lence.

157 H/L also informs computational flow models that use a Coulomb friction law,
158 including TITAN2D [Patra et al., 2005], which have built upon the work of Savage

159 and Hutter [1989], who used Coulomb friction laws in conjunction with depth-
160 averaged equations for mass and momentum. The Heim coefficient can therefore
161 provide a guideline for choosing appropriate basal friction input angles for differ-
162 ent flow volumes for TITAN2D [Ogburn, 2008, 2014, Charbonnier and Gertisser,
163 2012, Charbonnier et al., 2015].

164 LAHARZ and PFZ use semiempirical equations for planimetric area ($A_p =$
165 $cV^{2/3}$) and cross-sectional area ($A_{xs} = CV^{2/3}$) to predict lahar [Iverson et al.,
166 1998], debris flow, rock avalanche [Griswold and Iverson, 2008] and PDC [Widi-
167 wijayanti et al., 2008] inundation using empirically derived coefficients (c and C)
168 from a variety of mass flow deposits worldwide. These relationships also form the
169 basis of flow models using constant shear stress instead of constant friction [e.g.,
170 VolcFlow, Kelfoun and Druitt, 2005].

171 With increasing application of these respective flow modeling approaches, it
172 is now timely and appropriate to undertake more considered approaches to un-
173 derstanding and quantifying the uncertainty related to the use of mobility metrics
174 as model inputs. This work has been driven by our specific interest in constrain-
175 ing the basal friction input parameter required by TITAN2D when undertaking
176 ensemble runs for generating probabilistic hazards maps [Bayarri et al., 2009,
177 Spiller et al., 2014, Bayarri et al., 2015], by using the H/L -volume mobility rela-
178 tionships for block-and-ash flows from the FlowDat database. The application of
179 the method developed can, however, be applied widely.

180

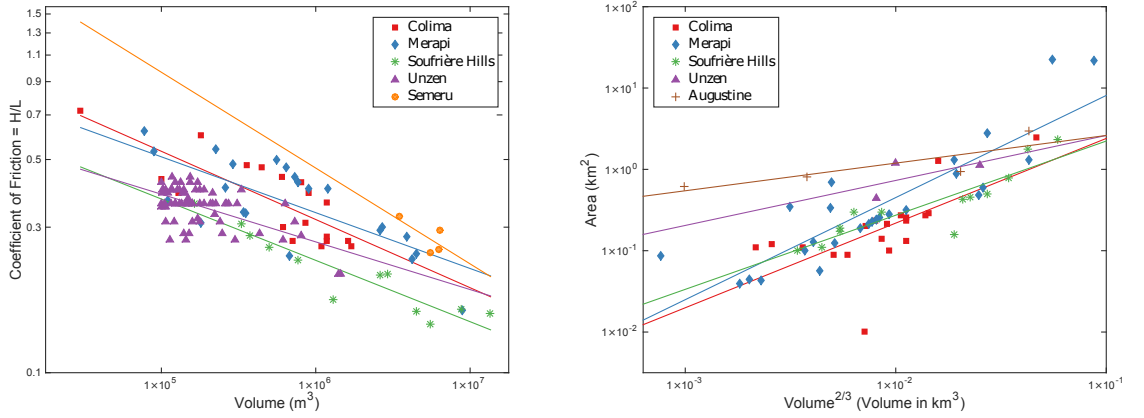


Figure 1: Data from all volcanoes considered for each of the two respective relationships along with their respective linear regression lines. Left: coefficient of friction (H/L) vs. volume (V) (both on a log scale). Colima, Merapi, SHV, and Unzen volcanoes have plentiful data, while data for Semeru is sparse. Right: planimetric area (A_p) vs. $V^{2/3}$ (both on a log scale). Colima, Merapi, and SHV have plentiful data, while data for Unzen and Semeru is sparse. Error bars on all values except volume are smaller than the markers themselves. Errors on volumes were only reported for SHV, which were often smaller than the marker itself. Note that not all PDCs had both (H/L) and (A_p) values reported in the literature.

181 3 Statistical analyses

182 Herein, we present a method using hierarchical Bayes modeling to leverage the
 183 global record of mobility metrics for PDCs, which can aid in cases where data
 184 for a particular volcano is sparse. We use the FlowDat database of mass flow
 185 mobility metrics [Ogburn, 2012b, 2014], which is current through 2014. From
 186 FlowDat [Ogburn, 2012b], 4 volcanoes were selected with plentiful (14 to 80
 187 flows) H/L , planimetric area, and volume data for dome-collapse PDCs: Col-

188 ima volcano, Mexico [data from: Saucedo et al., 2002, 2004, 2010]; Merapi,
 189 Indonesia [data from: Boudon et al., 1993, Bourdier and Abdurachman, 2001,
 190 Schwarzkopf et al., 2005, Charbonnier and Gertisser, 2011, Charbonnier et al.,
 191 2013, Komorowski et al., 2013]; Soufrière Hills Volcano, Montserrat [data from:
 192 Calder et al., 1999, Cole et al., 2002, Hards et al., 2008, Komorowski et al., 2010,
 193 Loughlin et al., 2010, Cole et al., 2014]; and Unzen, Japan [data from: Nakada
 194 et al., 1999, Takarada, 2008] (figure 1). Volcanoes with sparse data are also used:
 195 Semeru, Indonesia (for the (H/L) plot) [data from: Thouret et al., 2007]; and
 196 Augustine, Alaska [data from: Kamata et al., 1991, Vallance et al., 2010, Global
 197 Volcanism Program, 2013], and Unzen, Japan [data from: Nakada et al., 1999]
 198 for the $(A_p$ vs. $V^{2/3}$ plot). These flows are all dense, concentrated dome-collapse
 199 PDCs (block and ash flows), for which it is reasonable to assume broadly similar
 200 flow behavior. Error was rarely reported by the sources of the data, but is shown
 201 as error bars where available. However, the error bars were often smaller than the
 202 markers themselves.

203 For the frictional model of mobility (H/L vs. V), the strong linear relationship
 204 between the logarithm of PDC volume and the logarithm of the coefficient of
 205 friction (discussed in section 2) suggests the use of a linear model, such as a
 206 regression model

$$y = \alpha + \beta x + \epsilon, \quad \epsilon \stackrel{iid}{\sim} N(0, \sigma^2)$$

207 where x is the log-volume¹, y is the log-coefficient of friction (H/L), α and β are

¹Actually $x = \log_{10}(\text{volume}/10^{5.5})$. This x -origin then corresponds volume of $10^{5.5}\text{m}^3$, roughly where the slope and intercept are least correlated.

208 the intercept and slope of the regression line, and ϵ is random error. Graphically,
209 this model would correspond to fitting a straight line through all of the data \mathbf{y}
210 in figure 1 which minimizes the errors between estimated and observed values.
211 This approach corresponds to one end-member option, that is, to assume that the
212 relationship between the coefficient of friction and flow volume for block-and-ash
213 flows is constant at every volcano, and thus use information from all the volcanoes
214 to fit a regression.

215 Alternatively, one could fit separate regression lines for each of the J volca-
216 noes, namely

$$y_j = \alpha_j + \beta_j x + \epsilon, \quad \epsilon \stackrel{iid}{\sim} N(0, \sigma_j^2),$$

217 based on the data \mathbf{y}_j from volcano j alone. The result of separate regression
218 fits is shown in figure 1. This approach represents the alternative end-member
219 option, that is, to assume that the relationship between the coefficient of friction
220 and volume at different volcanoes is unrelated and thus use only the information
221 from a given volcano to fit a regression.

222 Likewise, to fit the constant resisting shear stress relationship (A_p vs. $V^{2/3}$),
223 we apply the same models to the transformed volume and planimetric area data
224 by letting x be the $\log-V^{2/3}$ and y be the \log -planimetric area (A_p). The anal-
225 ysis in the next section is described in terms of the frictional relationship, but
226 applied in an identical manner for the constant resisting shear stress relationship
227 using the appropriate definitions for x and y . Furthermore, the hierarchical anal-
228 ysis presented in the next section could prove useful for *any* linear relationship

229 suggested by transformations of volcanic datasets – the frictional and constant re-
230 sisting shear stress relationships for dome-collapse PDCs used here are just two
231 pertinent examples.

232 **3.1 Hierarchical Bayesian model**

233 In situations such as this, where it is unclear whether to fit an overall regres-
234 sion or separate regressions, it has become common statistical practice to use the
235 hierarchical or multilevel approach, which is a happy medium between these end-
236 member alternatives. Hierarchical modeling is carried out via Bayesian analysis,
237 wherein a *prior* probability distribution is chosen to describe knowledge about the
238 unknown model parameters (here the various regression parameters); this distri-
239 bution will then be updated by the data to form *posterior* probability distributions
240 of the unknown model parameters.

241 The version of hierarchical modeling that we utilize here links together the
242 separate regressions by assuming that the regression line slopes arose from the
243 common normal distribution (part of the prior distribution)

$$\beta_j \text{ are i.i.d. } N(\mu, \tau^2),$$

244 with unknown hyper-mean (the mean of the prior distribution) μ and hyper-variance
245 (the variance of the prior distribution) τ^2 . Note that, if $\tau^2 = 0$, then all the β_j
246 would be equal, so we would be back to the case of a single regression. At the
247 other extreme, as $\tau^2 \rightarrow \infty$, this model would yield the same answers as the sep-

248 arate regression models. The performance of the hierarchical model, in situations
249 such as this, is typically better than that of either of the two extremes.

250 Initially we will presume that little is known about μ and τ^2 (a vague prior dis-
251 tribution will be used for these parameters), but we will learn about them from the
252 data through their posterior distribution and they, in turn, will affect the posterior
253 distribution of the β_j .

254 If data were plentiful at each volcano, there would be little need (but also no
255 harm) in employing the hierarchical model, as the effect of the posterior distri-
256 bution of μ and τ^2 on the β_j would then be minimal. When data is sparse for
257 one or more volcanoes, however, the gains with the hierarchical approach can be
258 considerable. For instance, from the left panel of figure 1 it can be seen that there
259 are only four data points from Semeru for a very narrow range of PDC volumes,
260 and attempting to fit a separate regression to just four points will lead to a very
261 uncertain result. In contrast, the hierarchical modeling approach allows for ‘bor-
262 rowing strength’ from the other volcanoes in estimating Semeru’s regression line
263 slope (because of the assumption that all slopes arose from a common normal
264 distribution), and will be seen to result in much tighter credible intervals for the
265 regression line for Semeru.

266 To complete the specification of the hierarchical model, we need to also choose
267 ‘prior’ distributions for the other unknown parameters in the model. Whereas the
268 regression coefficients from figure 1 appear quite related, the intercepts, α_j , seem
269 considerably more variable. We could utilize a hierarchical model for the inter-
270 cepts but, since there will be little gain, we instead employ an objective constant

271 prior distribution $\pi^O(\alpha_1, \dots, \alpha_J) = 1$; although this objective prior does not in-
272 duce any sharing of intercept information across volcanoes, the changes in the
273 slope parameters through their hierarchical modeling will influence the intercepts.

274 In developing prior distributions for the regression variances σ_j^2 , it is important
275 to consider that the PDC data represented in figure 1 contain data from both highly
276 channelized and unchannelized (unconfined) flows, which experience different
277 frictional forces and exhibit different mobilities [Ogburn, 2014, Charbonnier and
278 Gertisser, 2011, Stinton, 2014]. Modeling by Stinton [2014] using TITAN2D
279 showed that flows confined in synthetic channels had longer runouts, higher ve-
280 locities, and shorter travel times than flows simulated over synthetic unconfined
281 terrain. Lube et al. [2011] found a similar topographic effect on the A_p vs. $V^{2/3}$
282 metric, as increasing the proportion of the flow which escaped from a channel
283 strongly increased this ratio. This was explained by the order of magnitude dif-
284 ference between the thickness of channel-confined and unconfined portions of the
285 deposits. Lube et al. [2011] and Charbonnier and Gertisser [2011] also noted a
286 change in mobility metrics as flows inundating the same drainage progressively
287 filled and reduced the carrying capacity of the channel, resulting in higher pro-
288 portions of unconfined deposits. The degree of channelization of particular PDCs
289 is not trivial to determine in a quantitative sense, as PDCs often exhibit a combi-
290 nation of both channelized and unchannelized transport that varies downstream.
291 Additionally, many of the traditional metrics (i.e. plan aspect ratio) can be heavily
292 influenced by the width, and thus confinement imposed by, of the channels them-
293 selves (see [Ogburn, 2014]). However, both qualitative descriptions of PDCs from

294 the literature and transect measurements of channelization for a limited number
295 of PDCs indicate that both the Merapi and Colima datasets contain PDCs with
296 lower degrees of channelization than the datasets from the other three volcanoes.
297 PDCs at Merapi and Colima also tend to inundate multiple channels, while those
298 elsewhere typically travel down a single channel.

299 These differences are also apparent in the data. Indeed, Table 1 gives the re-
300 sults of separate regressions at the five volcanoes, and the mean square residual
301 (MSR) are very similar for the three volcanoes with dominantly channelized flows
302 and much smaller than the MSR for the volcanoes with dominantly unchannelized
303 flow deposits. The higher MSR for unchannelized flows or those that inundate
304 multiple channels makes intuitive sense, as these flows travel over extremely var-
305 ied topography, with greater variation in slope and surface roughness than flows
306 which travel down channels. The one exception are PDCs at Augustine, which
307 were mainly unchannelized, but each PDC was emplaced over relatively similar
308 substrates of snow and ice, reflected in the low MSR for those flows. We have,
309 therefore, grouped it with the channelized flows.

Table 1: Linear regression parameters and MSR for each volcano for H/L vs. V
relationship. The (*) marks volcanoes with flows which are generally
310 **unchannelized.**

Volcano	Lin. Reg. Slope	Lin. Reg. Intercept	MSR ($\times 10^{-4}$)
Colima*	-0.224	-0.386	66.5
Merapi*	-0.183	-0.384	95.2
SHV	-0.201	-0.531	24.8
Unzen	-0.156	-0.493	26.3
Semeru	-0.314	-0.172	24.3

311

312 Therefore, it would be natural to have a separate variance for the channelized
313 and the unchannelized flow data. We, thus, assign Merapi and Colima a common
314 variance σ_C^2 and the other volcanoes common variance σ_U^2 , with the two variances
315 being unknown.

316 The equivalent slope, intercept, error information for the A_p vs. $V^{2/3}$ rela-
317 tionship is summarized in Table 2. For this analysis, we also apply the channel-
318 ized/unchannelized grouping to specify σ_C^2 and σ_U^2 .

Table 2: Linear regression parameters and MSR for each volcano for the A_p vs. $V^{2/3}$ relationship. The (*) marks volcanoes with flows which are generally **unchannelized**, see text for explanation about Augustine PDCs.

319

Volcano	Lin. Reg. Slope	Lin. Reg. Intercept	MSR
Colima*	1.041	1.421	0.142
Merapi*	1.256	2.165	0.128
SHV	0.912	1.260	0.042
Unzen	0.553	0.971	0.076
Augustine*	0.340	0.757	0.039

320

321 To complete the Bayesian model, prior distributions are needed for σ_C^2 and
 322 σ_U^2 and for the hyperparameters μ and τ^2 from the hierarchical prior. For these
 323 parameters we utilize a standard objective prior – called the *reference prior* –
 324 $\pi^R(\mu, \sigma_\beta^2, \sigma_C^2, \sigma_U^2)$; this is given in Appendix B. The reference prior is chosen so
 325 as to minimize the influence of the prior distribution on the analysis, i.e., to ensure
 326 that the posterior distribution of the model parameters only reflects what the data
 327 has to say.

328 This completes the specification of the Bayesian hierarchical model, and one
 329 now simply applies Bayes theorem to obtain the posterior distribution of all un-
 330 knowns parameters, given all the data \mathbf{y} , as

$$\begin{aligned} \pi(\alpha_1, \dots, \alpha_J, \beta_1, \dots, \beta_J, \mu, \tau^2, \sigma_C^2, \sigma_U^2 \mid \mathbf{y}) &\propto \prod_{j=1}^J f(\mathbf{y}_j \mid \alpha_j, \beta_j, \sigma_j^2) \\ &\times \pi^O(\alpha_1, \dots, \alpha_J) \pi^R(\mu, \sigma_\beta^2, \sigma_C^2, \sigma_U^2) \prod_{j=1}^J N(\beta_j \mid \mu, \tau^2), \end{aligned} \quad (1)$$

331 where $f(\mathbf{y}_j \mid \alpha_j, \beta_j, \sigma_j^2)$ is the likelihood arising from the data at volcano j and
 332 the σ_j^2 are either the channelized or unchannelized variance.

333 3.2 Analysis

334 There are no closed form analytical expressions for estimates of unknown pa-
 335 rameters or for credible intervals, but there is a relatively straightforward Markov
 336 Chain Monte Carlo (MCMC) method – described in Appendix B – for drawing

337 samples from the posterior distribution in (1). From this set of samples,

$$\{(\alpha_1^i, \dots, \alpha_J^i, \beta_1^i, \dots, \beta_J^i, \mu^i, (\tau^2)^i, (\sigma_C^2)^i, (\sigma_U^2)^i), \quad i = 1, \dots, m\},$$

338 all desired inferences can be performed.

339 The typical parameter estimate would be the posterior mean, computed as the
340 average of all of the samples; enough samples are typically chosen ($m = 10^6$ was
341 used in the computations herein) that the numerical error in this computation is
342 negligible. Similarly a 95% credible interval, for example, would be formed as the
343 interval containing the central 95% of the ordered sample. Even more informa-
344 tively, the entire posterior distribution of a parameter could be approximated by
345 simply making a histogram of the sample values. These histograms are illustrated
346 in Appendix B (figure 5 and figure 6). Note, in particular, from figure 6 that the
347 channelized and unchannelized variances do seem to be quite different.

348 Next, we turn to use of the regression samples to draw the desired geophysical
349 conclusions.

350 **4 Geophysical Results and Discussion**

351 The coefficient of friction - volume relationship can be studied in several ways
352 from the posterior sample of parameters. Thus, for volcano j , we have a sam-
353 ple $\{(\alpha_j^i, \beta_j^i), \quad i = 1, \dots, m\}$ of the intercepts and slopes. We thus immediately
354 have a sample from the posterior distribution of all regressions lines, illustrated in

355 figure 2.

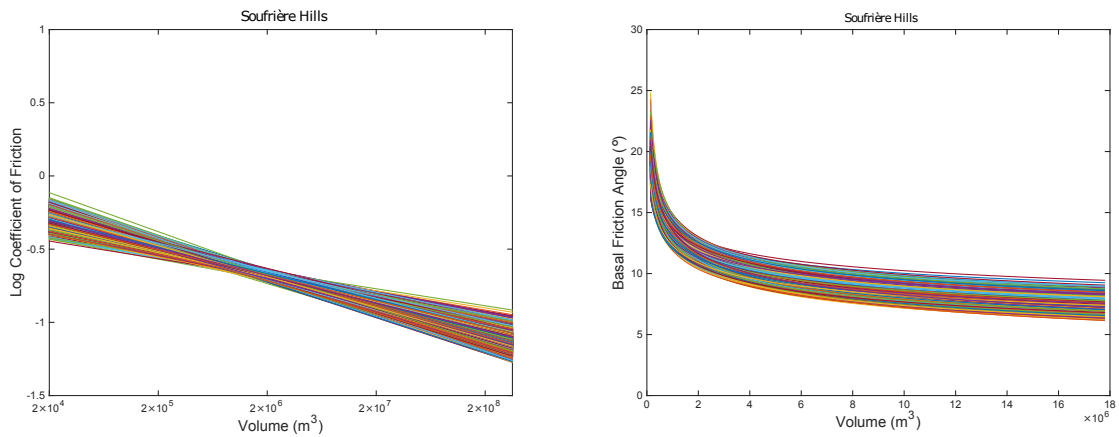


Figure 2: Both figures represent samples from the hierarchical linear regression model of the frictional relationship applied to the data, but show the same sample curves on different scales. Left: coefficient of friction and volume each on a log scale (which the linear model was fit to), Right: Basal friction angle (calculated as \arctan of the coefficient of friction) versus volume on a linear scale ($1 \times 10^6 \text{m}^3$).

356

357 Samples of regression lines are useful for the computation of inundation prob-
358 abilities from PDCs; for example, where it is necessary to consider different pos-
359 sible mobilities for flows over a range of volumes. Samples from regression lines
360 can be used directly for empirical models such as the energy line/cone method
361 or for estimating the basal friction input parameter for a geophysical model like
362 TITAN2D [Bayarri et al., 2009, Ogburn, 2014, Spiller et al., 2014] or the constant
363 resisting shear stress input parameter in VolcFlow [Ogburn, 2014]. Furthermore,
364 using regression samples generated by this method allows one to account for un-
365 certainty in probabilistic assessments of PDC inundation.

366 Figure 3 gives, for each volcano, a posterior summary consisting of the regres-
367 sion line corresponding to the posterior median values of the sample regression
368 lines (the solid red line) – this would be the natural estimated regression line from
369 the Bayesian analysis. 95% credible intervals (the dashed red lines) are also shown
370 and are obtained, at each volume value V , by taking the central 95% interval of
371 values of $\alpha_j^i + \beta_j^i \log_{10}(V)$, over the posterior samples.

372 For comparison, the confidence intervals on the regression function from clas-
373 sical individual regressions are also given in figure 3, with the solid black line
374 being the standard estimated regression function and the dashed black lines being
375 the standard 95% confidence intervals. As expected, for the volcanoes with abun-
376 dant data, there is not much difference between the hierarchical model regression
377 summaries and the classical regressions. But, for Semeru, which had only four
378 data points all of which are closely clustered in volume, the differences found
379 would affect the results of a probabilistic analyses, with the hierarchical approach
380 providing tighter uncertainty estimates. This conclusion is, of course, predicated
381 on the scientific judgment that the slope of the Semeru regression line is related to
382 the slopes of the others, but this is reasonable.

383 For the A_p vs. $V^{2/3}$ relationship, again we summarize the posterior distri-
384 bution of the hierarchical linear model. Figure 4 gives, for each volcano, the
385 regression line corresponding to the posterior median values of the sample regres-
386 sion lines (the solid red line), and 95% credible intervals (the dashed red lines)
387 formed, at each volume value V , by taking the central 95% interval of values of
388 $\alpha_j^i + \beta_j^i \log_{10}(V)$, over the posterior samples. And again, for comparison, the con-

389 fidence intervals on the regression function from classical individual regressions
390 are also given, with the solid black line being the standard estimated regression
391 function and the dashed black lines being the standard 95% confidence intervals.

392 Again, for figure 4 we have two volcanoes with limited data, Unzen (three
393 data points) and Augustine (four data points). The reduction in uncertainty ob-
394 tained through the hierarchical linear model is rather different for the two cases.
395 Although the 95% credible intervals from the hierarchical model are reduced in
396 both cases (as well as for Colima), the improvements are much starker for Unzen,
397 which has data points that are tightly clustered in volume. This is a case, much
398 like Semeru in the frictional relationship, where “borrowing strength” from other
399 volcanoes via the hierarchical analysis greatly reduces uncertainty in fitting an
400 inferential relationship.

401 This type of approach is broadly applicable to other types of mass flows (debris
402 avalanches, lahars, or column-collapse PDCs, for example) or other types of data
403 entirely (ash-dispersion metrics, for example), but it is important that the datasets
404 selected describe phenomena that are similar. This work focused only on dense,
405 dome-collapse PDCs which are considered to have broadly similar emplacement
406 dynamics; and accounted for dissimilarities (i.e. differences in channelization)
407 by allowing for different variances. However, the more similar the phenomena
408 at different volcanoes, the better the method is able to reduce uncertainty. The
409 selection of appropriate data is thus subject to scientific judgment.

410 Finally, it is important to note that this work does not seek to recommend one
411 mobility metric over another, but rather to illustrate the usefulness of the hierarchi-

412 cal Bayesian approach for different types of commonly reported mobility metrics
413 that inform model inputs. The choice of which mobility metric, conceptual model,
414 or computational model is most appropriate for different types of mass flows is a
415 matter of much debate [e.g Dade and Huppert, 1998, Kilburn and Sørensen, 1998,
416 Legros, 2002, Kelfoun and Druitt, 2005] and detailed comparisons of these models
417 can be found elsewhere in the literature [Kelfoun and Druitt, 2005, Charbonnier
418 and Gertisser, 2012, Ogburn, 2014]. It is also worth noting here that for larger
419 volume and more dilute flows, fluidization and turbulence plays a more domi-
420 nant role and that the mobility metrics and modeling tools referred to here are of
421 limited utility.

422 **5 Conclusions**

423 Understanding the past behavior of a particular volcano is the foundation upon
424 which assessments of potential future hazards are based. However, complete and
425 robust datasets are very rare, and really only exist for a handful of very well-
426 studied volcanoes. Additionally, newly active volcanoes may produce hazards
427 with poorly constrained characteristics. This problem can be handled by: 1) using
428 only the data from a particular volcano (which may be sparse, and thus intro-
429 duces large uncertainties into hazard assessments); or 2) using the global record
430 of volcanoes (which may ignore or downplay any particularities of the volcano
431 in question). The hierarchical Bayesian method for analyzing mobility metrics
432 presented herein allows one to achieve a happy medium between these two ap-

433 proaches by not only using data from a particular volcano, but also “borrowing
 434 strength” from the global record of PDC behavior and thus greatly reducing the
 435 uncertainty for volcanoes with sparse data.

436 **6 Acknowledgments**

437 The authors would like to thank two anonymous reviewers and editor Charles
 438 Connor for their helpful reviews and feedback. This work was supported in part
 439 by the following grants: NSF EAR-0809543 NSF NERC RiftVolc NE/L013932/1
 440 and NSF EAR-1331353

441 **Appendix A**

Table 3: Variables and abbreviations.

<i>Frictional model</i>	
V	volume of PDC
H	height dropped/vertical travel distance of PDC
L	runout length of PDC
H/L	Heim coefficient, coefficient of friction in the friction model
<i>Constant resisting shear stress model</i>	
A_p	Planimetric area of PDC inundation
A_{xs}	Cross-sectional area of PDC

<i>Statistical model</i>	
y	dependent variable: log-coefficient of friction (H/L), or planimetric area
x	independent variable: log-volume or $V^{2/3}$
α	intercept of the regression line
β	slope of the regression line
ϵ	random error
<i>iid</i>	is independent and identically distributed
\sim	has the distribution
$N(0, \sigma^2)$	a normal distribution with a mean of 0 and a variance σ^2
J	each of the J volcanoes
μ	hyper-mean, the mean of the prior distribution
τ^2	hyper-variance, the variance of the prior distribution
$\pi^O(\alpha_a, \dots, \alpha_J) = 1$	objective constant prior distribution
σ_C^2	common variance for channelized PDCs
σ_U^2	common variance for unchannelized PDCs
$\pi^R(\mu, \sigma_\beta^2, \sigma_C^2, \sigma_U^2)$	reference prior
MSR	Mean square residual
MCMC	Markov Chain Monte Carlo

442 **Appendix B**

443 The technical details of the hierarchical Bayesian analysis are given herein. First,
 444 some notation: write the design matrix for the j^{th} regression (i.e., the intercept
 445 constant 1 and the transformed volume input values) as (with n_j being the number
 446 of observations for Volcano j)

$$\mathbf{X}_j = \begin{pmatrix} 1 & x_{j1} \\ 1 & x_{j2} \\ \vdots & \vdots \\ 1 & x_{jn_j} \end{pmatrix},$$

and define (recalling that the σ_j^2 are σ_C^2 or σ_U^2 for the channelized and unchannel-
 ized volcanoes)

$$\bar{x}_j = \frac{1}{n_j} \sum_{i=1}^{n_j} x_{ji}, \quad S_j = \sum_{i=1}^{n_j} (x_{ji} - \bar{x}_j)^2, \quad \lambda_j = \frac{\tau^2}{\sigma_j^2}, \quad v_j = v_j(\sigma_j^2, \tau^2) = d_j + \tau^2, \quad d_j = \frac{\sigma_j^2}{S_j},$$

$$\mathbf{v} = (v_1, \dots, v_J), \quad n = \sum_{j=1}^J n_j, \quad \begin{pmatrix} \hat{\alpha}_j \\ \hat{\beta}_j \end{pmatrix} = (\mathbf{X}'_j \mathbf{X}_j)^{-1} \mathbf{X}'_j \mathbf{y}_j, \quad \hat{\boldsymbol{\mu}}(\mathbf{v}) = \frac{\sum_{j=1}^J \hat{\beta}_{j2}/v_j}{\sum_{j=1}^J 1/v_j}.$$

447 The objective reference prior for the parameters $(\mu, \tau^2, \sigma_U^2, \sigma_C^2)$ is [Berger and
 448 Bernardo, 1992]

$$\pi(\mu, \tau^2, \sigma_U^2, \sigma_C^2) = \left(\frac{1}{\sigma_U^2 \sigma_C^2} \right) \sqrt{\sum_{j=1}^J \frac{1}{v_j^2(\sigma_j^2, \tau^2)}}.$$

449 Then a Gibbs sampler [Casella and George, 1992] can be constructed as follows,
 450 to draw samples from the posterior distribution in (1).

451 **Step 1.** Draw the β_j , given σ_j^2 , μ and τ^2 , from the following distribution:

$$N \left(\hat{\beta}_j - \frac{(\hat{\beta}_j - \mu)}{1 + \lambda_j S_j}, \frac{\sigma_j^2 \lambda_j}{1 + \lambda_j S_j} \right).$$

452 This is the marginal posterior distribution of β_j , given σ_j^2 , μ and τ^2 (i.e., α_j
 453 has been integrated out). Note that we could have also integrated out μ , but
 454 that should not be necessary because below we generate μ from its marginal
 455 posterior distribution with the β s integrated out.

456 **Step 2.** Draw the α_j , given σ_j^2 and β_j , from the $N(\hat{\alpha}_j - \bar{x}_j(\beta_j - \hat{\beta}_j), \sigma_j^2/n_j)$
 457 distribution. This is the conditional posterior distribution of α_j , given σ_j^2
 458 and β_j . (It happens to not depend on τ^2 or μ .)

459 **Step 3A.** Propose a value of σ_U^2 , given the $\{\beta_j\}, j = 1, 2$, by drawing a random
 460 variable from the inverse gamma distribution with shape parameter $\alpha_U =$
 461 $(n_1 + n_2)/2$ and rate parameter

$$\beta_U = \frac{1}{2} \sum_{j=1}^2 (y_{ji} - [\alpha_j + x_{ji}\beta_j])^2.$$

462 Draw a uniform random variable U on $(0, 1)$ and accept the proposed σ_U^2 if

$$U < \frac{\sqrt{\sum_{j=1}^J 1/v_j^2(\sigma_j^2, \tau^2)}}{\sqrt{\sum_{j=1}^2 1/v_j^2(0, \tau^2) + \sum_{j=3}^5 1/v_j^2(\sigma_j^2, \tau^2)}};$$

463 else discard σ_U^2 and propose a new σ_U^2 , repeating as necessary until a σ_U^2
 464 is accepted. This arises from the standard accept-reject algorithm because
 465 the numerator above, which is the unnormalized ratio of the target posterior
 466 distribution and the inverse gamma proposal distribution, is maximized at
 467 $\sigma_U^2 = 0$.

468 **Step 3B.** Propose a value of σ_C^2 , given the $\{\beta_j\}$, $j = 3, 4, 5$, by drawing a random
 469 variable from the inverse gamma distribution with shape parameter $\alpha_C =$
 470 $(n_3 + n_4 + n_5)/2$ and rate parameter

$$\beta_C = \frac{1}{2} \sum_{j=3}^5 (y_{ji} - [\alpha_j + x_{ji}\beta_j])^2.$$

471 Draw a uniform random variable U on $(0, 1)$ and accept σ_C^2 if

$$U < \frac{\sqrt{\sum_{j=1}^J 1/v_j^2(\sigma_j^2, \tau^2)}}{\sqrt{\sum_{j=1}^J 1/v_j^2(\sigma_j^2, \tau^2) + \sum_{j=3}^5 1/v_j^2(0, \tau^2)}};$$

472 else discard σ_C^2 and draw a new σ_C^2 , repeating as necessary until a σ_C^2 is
 473 accepted. The rationale is as in Step 3A.

474 These steps yield draws from the conditional posterior distributions of σ_U^2
 475 and σ_C^2 , given the $\{\alpha_j, \beta_j\}$, and do not depend on the other parameters.

476 **Step 4.** Draw μ , given the σ_j^2 and τ^2 , from the following distribution:

$$N\left(\hat{\mu}(\mathbf{v}), \frac{1}{\sum_{j=1}^J 1/v_j}\right).$$

477 This is the marginal posterior distribution of μ , given the σ_j^2 and τ^2 , i.e., all
478 the β s have been integrated out.

479 **Step 5.** Generate τ^2 , given μ , the $\{\beta_j\}$ and the σ_j^2 , by the following accept-reject
480 algorithm:

- 481 • Generate τ^2 from the inverse gamma distribution with shape parameter
482 $\alpha = (J - 2)/2$ and rate parameter $\beta = \frac{1}{2} \sum_{j=1}^J (\beta_j - \mu)^2$.
- 483 • Draw a uniform random variable U on $(0, 1)$ and accept τ^2 if

$$U < \frac{\sqrt{\sum_{j=1}^J 1/v_j^2(\sigma_j^2, \tau^2)}}{\sqrt{\sum_{j=1}^J 1/v_j^2(\sigma_j^2, 0)}};$$

484 else discard τ^2 and draw a new τ^2 , repeating as necessary until a τ^2 is
485 accepted.

486 This algorithm follows from noting that the likelihood for τ^2 , given all the
487 other parameters, is proportional to the given inverse gamma distribution.
488 The posterior distribution of τ^2 , given all the other parameters, is then pro-
489 portional to this likelihood times the prior; a sample is then drawn from this
490 posterior using accept/reject with the likelihood as the proposal distribution.

491 To “view” samples from the posterior and assess that the MCMC algorithm
492 is behaving properly [Mengersen et al., 1999], we consider histograms and trace
493 plots, respectively. Trace plots illustrate the entire sequence of samples from the
494 posterior distribution, or chain, (after the first few thousand are discarded) with the

495 value of the random variable plotted on the vertical axis vs. the sequence index.
496 The reader unfamiliar with MCMC sampling should note that a well-mixing algo-
497 rithm should not get “stuck” at one value for many samples, should not have too
498 many vertical outliers, and should not have a discernible periodic envelope. Note,
499 the samples (and trace plots) have been “thinned” keeping every fifth sample from
500 the MCMC sequence.

501 Of particular interest are slope parameters for each volcano, β_j , illustrated for
502 the frictional model in figure 5. Histograms of slope parameter samples for each
503 volcano give reassurance that we are sampling around a common slope, near -0.2 .
504 Spread in each individual histogram reflects the uncertainty of the slope parameter
505 for each volcano. Of course, wider histograms indicate more uncertainty.

506 Samples for *any* of the unknown parameters described by the posterior dis-
507 tribution can be visualized in this manner. For example, one might be interested
508 in estimating the inferential variance parameters for the two flow categorizations,
509 channelized vs. unchannelized. Descriptive illustrations of these samples are pre-
510 sented in figure 6. Of course, which unknown parameters are of particular interest
511 is dependent on the scientific questions at hand for a given problem.

512

513 **References**

514 I. Alberico, L. Lirer, P. Petrosino, and R. Scandone. A methodology for the evalu-
515 ation of long-term volcanic risk from pyroclastic flows in Campi Flegrei (Italy).

516 *Journal of Volcanology and Geothermal Research*, 116(1–2):63–78, 2002. doi:
517 10.1016/S0377-0273(02)00211-1.

518 F. Alfano, C. Bonadonna, A. C. M. Volentik, C. B. Connor, S. F. L. Watt, D. M.
519 Pyle, and L. J. Connor. Tephra stratigraphy and eruptive volume of the May,
520 2008, Chaitén eruption, Chile. *Bulletin of Volcanology*, 73(5):613–630, 2011.
521 doi: 10.1007/s00445-010-0428-x.

522 G. M. Allenby, P. E. Rossi, and R. E. McCulloch. Hierarchical Bayes models: A
523 practitioners guide, 2005. URL <http://ssrn.com/abstract=655541>.
524 Available at SSRN 655541.

525 M. Bayarri, J. Berger, E. Calder, K. Dalbey, S. Lunagomez, A. Patra, E. Pit-
526 man, E. Spiller, and R. Wolpert. Using statistical and computer models
527 to quantify volcanic hazards. *Technometrics*, 51(4):402–413, 2009. doi:
528 10.1198/TECH.2009.08018.

529 M. J. Bayarri, J. O. Berger, E. S. Calder, A. K. Patra, E. B. Pitman, E. T. Spiller,
530 and R. L. Wolpert. Probabilistic quantification of hazards: a methodology using
531 small ensembles of physics-based simulations and statistical surrogates. *Inter-
532 national Journal for Uncertainty Quantification*, 5(4):297–325, 2015. ISSN
533 2152-5080. doi: 10.1615/Int.J.UncertaintyQuantification.2015011451. URL
534 <http://www.dl.begellhouse.com/journals/52034eb04b657aea,6976a15960>

535 J. E. Begét and A. J. Limke. Two-dimensional kinematic and rheological modeling

- 536 of the 1912 pyroclastic flow, Katmai, Alaska. *Bulletin of Volcanology*, 50(3):
537 148–160, 1988. doi: 10.1007/BF01079679.
- 538 J. O. Berger and J. M. Bernardo. Reference priors in a variance components
539 problem. In P. K. Goel and N. S. Iyengar, editors, *Bayesian Analysis in Statistics
540 and Econometrics*, volume 75 of *Lecture Notes in Statistics*, pages 177–194.
541 Springer, New York, NY, 1992. ISBN 978-0-387-97863-5.
- 542 G. Boudon, G. Camus, A. Gourgaud, and J. Lajoie. The 1984 nuée-ardente de-
543 posits of Merapi volcano, Central Java, Indonesia: stratigraphy, textural char-
544 acteristics, and transport mechanisms. *Bulletin of Volcanology*, 55(5):327–342,
545 1993. doi: 10.1007/BF00301144.
- 546 J.-L. Bourdier and E. Abdurachman. Decoupling of small-volume pyroclastic
547 flows and related hazards at Merapi volcano, Indonesia. *Bulletin of Volcanol-
548 ogy*, 63(5):309–325, 2001. doi: 10.1007/s004450100133.
- 549 S. K. Brown, H. S. Crossweller, R. S. J. Sparks, E. Cottrell, N. I. Deligne, N. O.
550 Guerrero, L. Hobbs, K. Kiyosugi, S. C. Loughlin, L. Siebert, and S. Takarada.
551 Characterisation of the Quaternary eruption record: analysis of the Large Mag-
552 nitude Explosive Volcanic Eruptions (LaMEVE) database. *Journal of Applied
553 Volcanology*, 3:22, 2014. doi: 10.1186/2191-5040-3-5.
- 554 E. S. Calder, P. D. Cole, W. B. Dade, T. H. Druitt, R. P. Hoblitt, H. E. Huppert,
555 L. J. Ritchie, R. S. J. Sparks, and S. R. Young. Mobility of pyroclastic flows

- 556 and surges at the Soufrière Hills Volcano, Montserrat. *Geophysical Research*
557 *Letters*, 26(5):537–540, 1999. doi: 10.1029/1999GL900051.
- 558 L. Capra, V. C. Manea, M. Manea, and G. Norini. The importance of digital
559 elevation model resolution on granular flow simulations: a test case for Colima
560 volcano using TITAN2D computational routine. *Natural Hazards*, 59(2):665–
561 680, 2011. doi: 10.1007/s11069-011-9788-6.
- 562 G. Casella and E. I. George. Explaining the Gibbs sampler. *The American Statis-*
563 *tician*, 46(3):167–174, 1992. doi: 10.1080/00031305.1992.10475878.
- 564 S. J. Charbonnier and R. Gertisser. Numerical simulations of block-and-
565 ash flows using the Titan2D flow model: examples from the 2006
566 eruption of Merapi Volcano, Java, Indonesia. *Bulletin of Volcanol-*
567 *ogy*, 71(8):953–959, 2009. doi: 10.1007/s00445-009-0299-1. URL
568 <http://search.proquest.com/docview/898788673?accountid=13771>
569 <http://link.springer.com/10.1007/s00445-009-0299-1>.
- 570 S. J. Charbonnier and R. Gertisser. Deposit architecture and dynamics of the 2006
571 block-and-ash flows of Merapi Volcano, Java, Indonesia. *Sedimentology*, 58
572 (6):1573–1612, 2011. doi: 10.1111/j.1365-3091.2011.01226.x.
- 573 S. J. Charbonnier and R. Gertisser. Evaluation of geophysical mass flow
574 models using the 2006 block-and-ash flows of Merapi Volcano, Java,
575 Indonesia: Towards a short-term hazard assessment tool. *Journal of*

- 576 *Volcanology and Geothermal Research*, 231–232:87–108, 2012. doi:
577 10.1016/j.jvolgeores.2012.02.015.
- 578 S. J. Charbonnier, A. Germa, C. B. Connor, R. Gertisser, J.-C. Komorowski,
579 K. Preece, F. Lavigne, T. Dixon, and L. Connor. Evaluation of the im-
580 pact of the 2010 pyroclastic density currents at Merapi volcano from high-
581 resolution satellite imagery, field investigation and numerical simulations. *Jour-
582 nal of Volcanology and Geothermal Research*, 261:295–315, 2013. doi:
583 10.1016/j.jvolgeores.2012.12.021.
- 584 S. J. Charbonnier, J. L. Palma, and S. E. Ogburn. Application of ‘shallow-water’
585 numerical models for hazard assessment of volcanic flows: the case of TI-
586 TAN2D and Turrialba volcano (Costa Rica). *Revista Geologica de America
587 Central*, pages 107–128, 2015. doi: 10.15517/rgac.v0i52.19021.
- 588 P. Cole, P. Smith, A. Stinton, H. Odbert, M. Bernstein, J.-C. Komorowski, and
589 R. Stewart. Vulcanian explosions at Soufriere Hills Volcano, Montserrat be-
590 tween 2008 and 2010. In G. Wadge, R. Robertson, and B. Voight, editors,
591 *The eruption of Soufrière Hills Volcano, Montserrat, from 2000 to 2010*, vol-
592 ume 39, pages 93–111. Geological Society of London, Memoirs, 2014. doi:
593 10.1144/M39.5.
- 594 P. D. Cole, E. S. Calder, R. S. J. Sparks, A. B. Clarke, T. H. Druitt, S. R. Young,
595 R. A. Herd, C. L. Harford, and G. E. Norton. Deposits from dome-collapse and
596 fountain-collapse pyroclastic flows at Soufrière Hills Volcano, Montserrat. In

- 597 T. H. Druitt and B. P. Kokelaar, editors, *The eruption of Soufrière Hills Volcano,*
598 *Montserrat, from 1995 to 1999*, volume 21, pages 231–262. Geological Society
599 of London, Memoirs, 2002. doi: 10.1144/GSL.MEM.2002.021.01.11.
- 600 G. B. Crosta, S. Cucchiaro, and P. Frattini. Validation of semi-empirical rela-
601 tionships for the definition of debris-flow behavior in granular materials. In
602 D. Rickenmann and C.-L. Chen, editors, *Proceedings of the Third International*
603 *Conference on Debris-Flow Hazards Mitigation: Mechanics, Prediction and*
604 *Assessment, Davos, Switzerland*, pages 821–831. Millpress, Rotterdam, NL,
605 2003.
- 606 H. Crossweller, B. Arora, S. Brown, E. Cottrell, N. Deligne, N. Guerrero, L. Hobbs,
607 K. Kiyosugi, S. Loughlin, J. Lowndes, M. Nayembil, L. Siebert, R. Sparks,
608 S. Takarada, and E. Venzke. Global database on large magnitude explosive
609 volcanic eruptions (LaMEVE). *Journal of Applied Volcanology*, 1(4):13, 2012.
610 doi: 10.1186/2191-5040-1-4.
- 611 W. B. Dade and H. E. Huppert. Long-runout rockfalls. *Geology*, 26(5):803–806,
612 1998. doi: 10.1130/0091-7613(1998).
- 613 N. I. Deligne, S. G. Coles, and R. S. J. Sparks. Recurrence rates of large explosive
614 volcanic eruptions. *Journal of Geophysical Research*, 115(B6), 2010. ISSN
615 0148-0227. doi: 10.1029/2009JB006554.
- 616 R. V. Fisher and H.-U. Schmincke. *Pyroclastic Rocks*. Springer-Verlag, New York,
617 NY, 1984. ISBN 978-3-540-51341-4. doi: 10.1007/978-3-642-74864-6.

- 618 P. W. Francis and M. C. W. Baker. Mobility of pyroclastic flows. *Nature*, 270:
619 164–165, 1977. doi: 10.1038/270164a0.
- 620 C. Furlan. Extreme value methods for modelling historical series of large volcanic
621 magnitudes. *Statistical Modelling*, 10(2):113–132, 2010. ISSN 1471-082X.
622 doi: 10.1177/1471082X0801000201.
- 623 Geological Survey of Japan and the National Institute of Advanced In-
624 dustrial Science and Technology (AIST). Catalog of eruptive events
625 during the last 10,000 years in japan, version 2.2, 2013. URL
626 <https://gbank.gsj.jp/volcano/eruption/index.html>.
- 627 Global Volcanism Program. Volcanoes of the World, v. 4.4.0, 2013. URL
628 <http://dx.doi.org/10.5479/si.GVP.VOTW4-2013>.
- 629 J. P. Griswold and R. M. Iverson. Mobility and statistics and auto-
630 mated hazard mapping for debris flows and rock avalanches, 2008. URL
631 <http://pubs.usgs.gov/sir/2007/5276/>. U. S. Geological Survey
632 Scientific Investigations Report 2007–5276.
- 633 V. Hards, M. Strutt, S. De Angelis, G. Ryan, T. Christopher, T. Syers, and V. Bass.
634 Report to the Scientific Advisory Committee on activity at Soufrière Hills Vol-
635 cano Montserrat: April 2008. *Montserrat Volcano Observatory Open File Re-*
636 *port*, OFR 09-01, 2008.
- 637 J. N. Hayashi and S. Self. A comparison of pyroclastic flow and debris avalanche

- 638 mobility. *Journal of Geophysical Research B: Solid Earth*, 97(B6):9063–9071,
639 1992. doi: 10.1029/92JB00173V.
- 640 A. Heim. Bergsturz und Menschenleben. *Zürich Vierteljahrsschrift*, 77:218, 1932.
641 [English translation by N. A. Skermer, 1989. Landslides and human lives: Van-
642 couver, B.C., BiTech Publishers, 195p].
- 643 D. M. Hooper and G. S. Mattioli. Kinematic modeling of pyroclastic flows pro-
644 duced by gravitational dome collapse at Soufrière Hills Volcano, Montserrat.
645 *Natural Hazards*, 23(1):65–86, 2001. doi: 10.1023/A:1008130605558.
- 646 A. Höskuldsson and J. M. Cantagrel. Volcanic hazards in the surroundings of
647 Pico de Orizaba, eastern Mexico. *Natural Hazards*, 10(3):197–219, 1994. doi:
648 10.1007/BF00596142.
- 649 K. J. Hsü. Catastrophic debris streams (Sturtzstroms) generated by rockfalls. *Ge-*
650 *ological Society of America Bulletin*, 86(1):129–140, 1975. doi: 10.1130/0016-
651 7606(1975)86;129:CDSSGB;2.0.CO;2.
- 652 O. Hungr. Mobility of rock avalanches. *Report of the National Research Institute*
653 *for Earth Science and Disaster Prevention, Japan*, 46:11–20, 1990.
- 654 R. M. Iverson, S. P. Schilling, and J. W. Vallance. Objective delineation of lahar-
655 inundation hazard zones. *Geological Society of America Bulletin*, 110(8):972–
656 984, 1998. doi: 10.1130/0016-7606(1998)110;0972:ODOLIH;2.3.CO;2.
- 657 H. Kamata, D. Johnston, and R. Waitt. Stratigraphy, chronology, and character

- 658 of the 1976 pyroclastic eruption of Augustine volcano, Alaska. *Bulletin of*
659 *Volcanology*, 53(6):407–419, 1991. doi: 10.1007/BF00258182.
- 660 K. Kelfoun and T. H. Druitt. Numerical modelling of the emplacement of the
661 7500 BP Socompa rock avalanche, Chile. *Journal of Geophysical Research B:*
662 *Solid Earth*, 110(B12):B12202, 2005. doi: 10.1029/2005JB003758.
- 663 C. R. J. Kilburn and S.-A. Sørensen. Runout lengths of sturzstroms; the control of
664 initial conditions and of fragment dynamics. *Journal of Geophysical Research*
665 *B: Solid Earth*, 103(B8):17877–17884, 1998. doi: 10.1029/98JB01074.
- 666 K. Kiyosugi, C. Connor, R. S. J. Sparks, H. S. Crossweller, S. K. Brown, L. Siebert,
667 T. Wang, and S. Takarada. How many explosive eruptions are missing from the
668 geologic record? Analysis of the quaternary record of large magnitude explo-
669 sive eruptions in Japan. *Journal of Applied Volcanology*, 4(1):17, 2015. ISSN
670 2191-5040. doi: 10.1186/s13617-015-0035-9.
- 671 J.-C. Komorowski, Y. Legendre, T. Christopher, M. Bernstein, R. Stewart,
672 E. Joseph, N. Fournier, L. Chardot, A. Finizola, G. Wadge, R. Syers,
673 C. Williams, and V. Bass. Insights into processes and deposits of hazardous vul-
674 canian explosions at Soufrière Hills Volcano during 2008 and 2009 (Montser-
675 rat, West Indies). *Geophysical Research Letters*, 37(19):1–6, 2010. doi:
676 10.1029/2010GL042558.
- 677 J.-C. Komorowski, S. Jenkins, P. Baxter, A. Picquout, F. Lavigne, S. Charbon-
678 nier, R. Gertisser, K. Preece, N. Cholik, A. Budi-Santoso, and Surono. Parox-

- 679 ysmal dome explosion during the Merapi 2010 eruption: Processes and fa-
680 cies relationships of associated high-energy pyroclastic density currents. *Jour-*
681 *nal of Volcanology and Geothermal Research*, 261:260–294, 2013. doi:
682 10.1016/j.jvolgeores.2013.01.007.
- 683 T. P. Kover and M. F. Sheridan. Numerical models for pyroclastic flows of Mt.
684 Unzen, Japan (abstract), 1993. Geological Society of America, Abstracts with
685 programs 25, 268.
- 686 F. Legros. The mobility of long-runout landslides. *Engineering Geology*, 63(3–4):
687 301–331, 2002. doi: 10.1016/S0013-7952(01)00090-4.
- 688 S. Loughlin, R. Lockett, and G. Ryan. An overview of lava dome evolution,
689 dome collapse and cyclicity at Soufriere Hills Volcano, Montserrat, 2005-2007.
690 *Geophysical Research Letters*, 37:1–6, 2010. doi: 10.1029/2010GL042547.
- 691 G. Lube, S. J. Cronin, and J.-C. Thouret. Kinematic characteristics of pyroclastic
692 density currents at Merapi and controls on their avulsion from natural and engi-
693 neered channels. *Geological Society of America Bulletin*, 123(5-6):1127–1140,
694 2011. doi: 10.1130/B30244.1.
- 695 M. C. Malin and M. F. Sheridan. Computer-assisted mapping of pyro-
696 clastic surges. *Science*, 217(4560):637–640, 1982. doi: 10.1126/sci-
697 ence.217.4560.637.
- 698 A. L. Martin del Pozzo, M. Sheridan, D. Barrera, J. Lugo Hubp, and

- 699 L. Vázquez Selem. Potential hazards from Colima volcano, Mexico. *Geofísica*
700 *Internacional*, 34(4):363–376, 1995.
- 701 W. Marzocchi, L. Sandri, and J. Selva. BET_EF: a probabilistic tool for long- and
702 short-term eruption forecasting. *Bulletin of Volcanology*, 70(5):623–632, 2008.
703 ISSN 0258-8900. doi: 10.1007/s00445-007-0157-y.
- 704 W. Marzocchi, L. Sandri, and J. Selva. BET_VH: a probabilistic tool for long-term
705 volcanic hazard assessment. *Bulletin of Volcanology*, 72(6):705–716, 2010.
706 ISSN 0258-8900. doi: 10.1007/s00445-010-0357-8.
- 707 K. L. Mengersen, C. P. Robert, and C. Guihenneuc-Jouyaux. MCMC convergence
708 diagnostics: A review. In J. M. Bernardo, J. O. Berger, A. P. Dawid, and A. F. M.
709 Smith, editors, *Bayesian Statistics 6*, pages 415–440. Oxford University Press,
710 Prague, 1999. ISBN 0-19-850485-3.
- 711 H. Murcia, M. Sheridan, J. Macías, and G. Cortés. TITAN2D simulations
712 of pyroclastic flows at Cerro Machín Volcano, Colombia: Hazard implica-
713 tions. *Journal of South American Earth Sciences*, 29(2):161–170, 2010. doi:
714 10.1016/j.jsames.2009.09.005.
- 715 I. A. Nairn and S. Self. Explosive eruptions and pyroclastic avalanches from
716 Ngauruhoe in February 1975. *Journal of Volcanology and Geothermal Re-*
717 *search*, 3(1–2):39–60, 1978. doi: 10.1016/0377-0273(78)90003-3.
- 718 S. Nakada, H. Shimizu, and K. Ohta. Overview of the 1990–1995 eruption at

- 719 unzen volcano. *Journal of Volcanology and Geothermal Research*, 89(1):1–22,
720 1999. doi: 10.1016/S0377-0273(98)00118-8.
- 721 S. Ogburn, S. Loughlin, and E. Calder. The association of lava dome growth
722 with major explosive activity (vei 4): Domehaz, a global dataset. *Bulletin of*
723 *Volcanology*, 77:1–17, 2015. doi: DOI: 10.1007/s00445-015-0919-x.
- 724 S. E. Ogburn. Potential hazards at Soufrière Hills Volcano, Montserrat:
725 Northwards-directed dome-collapses and major explosive eruptions. Master’s
726 thesis, State University of New York at Buffalo, Buffalo, NY, 2008.
- 727 S. E. Ogburn. DomeHaz: Dome-forming eruptions database, 2012a. On Vhub at
728 <https://vhub.org/groups/domedatabase>.
- 729 S. E. Ogburn. FlowDat: Mass flow database, 2012b. On Vhub at
730 <https://vhub.org/groups/massflowdatabase>.
- 731 S. E. Ogburn. *Reconciling field observations of pyroclastic density currents with*
732 *conceptual and computational analogs using a GIS and a newly developed*
733 *global database*. PhD thesis, State University of New York at Buffalo, Buf-
734 falo, NY, 2014.
- 735 A. K. Patra, A. C. Bauer, C. C. Nichita, E. B. Pitman, M. F. Sheridan, and M. I.
736 Bursik. Parallel adaptive numerical simulation of dry avalanches over natu-
737 ral terrain. *Journal of Volcanology and Geothermal Research*, 139(1–2):1–21,
738 2005. doi: 10.1016/j.jvolgeores.2004.06.014.

- 739 R. Saucedo, J. Macías, M. Bursik, J. Mora, J. Gavilanes, and A. Cortes. Emplace-
740 ment of pyroclastic flows during the 1998-1999 eruption of Volcán de Col-
741 ima, México. *Journal of Volcanology and Geothermal Research*, 117:129–153,
742 2002.
- 743 R. Saucedo, J. Macías, and M. Bursik. Pyroclastic flow deposits of the 1991
744 eruption of Volcán de Colima, Mexico. *Bulletin of Volcanology*, 66(4):291–
745 306, 2004. doi: 10.1007/s00445-003-0311-0.
- 746 R. Saucedo, J. Macías, J. Gavilanes, J. Arce, J.-C. Komorowski, J. Gard-
747 ner, and G. Valdez-Moreno. Eyewitness, stratigraphy, chemistry, and
748 eruptive dynamics of the 1913 Plinian eruption of Volcán de Col-
749 ima, México. *Journal of Volcanology and Geothermal Research*, 191
750 (3-4):149–166, 2010. doi: 10.1016/j.jvolgeores.2010.01.011. URL
751 <http://linkinghub.elsevier.com/retrieve/pii/S0377027310000259>.
- 752 S. B. Savage and K. Hutter. The motion of a finite mass of granular material
753 down a rough incline. *Journal of Fluid Mechanics*, 199:177–215, 1989. doi:
754 10.1017/S0022112089000340.
- 755 A. E. Scheidegger. On the prediction of the release and velocity of catastrophic
756 rockfalls. *Rock Mechanics*, 5(4):231–236, 1973. doi: 10.1007/BF0130179.
- 757 E. Scheller. Beitrag zum Bewegungsverhalten grosser Berstürze. *Eclogae Geo-*
758 *logicae Helvetiae*, 64:195–202, 1971.

- 759 L. Schwarzkopf, H.-U. Schmincke, and S. Cronin. A conceptual model for block-
760 and-ash flow basal avalanche transport and deposition, based on deposit archi-
761 tecture of 1998 and 1994 Merapi flows. *Journal of Volcanology and Geothermal*
762 *Research*, 139(1-2):117–134, 2005. doi: 10.1016/j.jvolgeores.2004.06.012.
- 763 T. Sheldrake. Long-term forecasting of eruption hazards: A hierarchical
764 approach to merge analogous eruptive histories. *Journal of Volcanol-*
765 *ogy and Geothermal Research*, 286:15–23, 2014. ISSN 03770273. doi:
766 10.1016/j.jvolgeores.2014.08.021.
- 767 M. F. Sheridan. Emplacement of pyroclastic flows— a review. In C. E. Chapin
768 and W. E. Elston, editors, *Ash-Flow Tuffs*, pages 125–136. Geological Society
769 of America, Special Paper 180, Boulder, CO, 1979.
- 770 M. F. Sheridan and J. L. Macías. Estimation of risk probability for gravity-
771 driven pyroclastic flows at Volcán Colima, México. *Journal of Volcanol-*
772 *ogy and Geothermal Research*, 66(1–4):251–256, 1995. doi: 10.1016/0377-
773 0273(94)00058-O.
- 774 M. F. Sheridan and M. C. Malin. Application of computer-assisted mapping to
775 volcanic hazard evaluation of surge eruptions: Vulcano, Lipari, and Vesuvius.
776 *Journal of Volcanology and Geothermal Research*, 17(1–4):187–202, 1983.
777 doi: 10.1016/0377-0273(83)90067-7.
- 778 M. F. Sheridan, B. Hubbard, G. Carrasco-Núñez, and C. Siebe. Pyroclastic flow

- 779 hazard at Volcán Citlaltépetl. *Natural Hazards*, 33(2):209–221, 2004. doi:
780 10.1023/B:NHAZ.0000037028.89829.d1.
- 781 M. F. Sheridan, A. K. Patra, K. Dalbey, and B. Hubbard. Probabilistic digital
782 hazard maps for avalanches and massive pyroclastic flows using TITAN2D. In
783 *Stratigraphy and geology of volcanic areas*, pages 281–291. Geological Society
784 of Amer, 2010. doi: 10.1130/2010.2464(14).
- 785 L. Siebert, T. Simkin, and P. Kimberly. *Volcanoes of the World*. Smithsonian
786 Institution, Washington D.C and University of California Press, Berkeley, 2010.
- 787 R. S. J. Sparks. Grain size variations in ignimbrites and implications for the
788 transport of pyroclastic flows. *Sedimentology*, 23(2):147–188, 1976. doi:
789 10.1111/j.1365-3091.1976.tb00045.x.
- 790 E. Spiller, M. Bayarri, J. Berger, E. Calder., A. Patra, E. Pitman,
791 and R. Wolpert. Automating emulator construction for geophys-
792 ical hazard maps. *SIAM/ASA Journal on Uncertainty Quantifi-*
793 *cation*, 2(1):126–152, 2014. doi: 10.1137/120899285. URL
794 <http://epubs.siam.org/doi/abs/10.1137/120899285>.
- 795 A. J. Stinton. *Effects of changes in valley geomorphology on the behavior of*
796 *volcanic mass-flows*. PhD thesis, State University of New York at Buffalo,
797 Buffalo, NY, 2014.
- 798 S. Takarada, 2008. (personal communication).

- 799 J.-C. Thouret, F. Lavigne, H. Suwa, B. Sukatja, and Surono. Volcanic hazards
800 at Mount Semeru, East Java (Indonesia), with emphasis on lahars. *Bulletin of*
801 *Volcanology*, 70(2):221–244, 2007. doi: 10.1007/s00445-007-0133-6.
- 802 J. W. Vallance, K. F. Bull, and M. L. Coombs. Pyroclastic flows, lahars and mixed
803 avalanches generated during the 2006 eruption of Augustine Volcano. In J. A.
804 Power, M. L. Coombs, and J. T. Freymueller, editors, *The 2006 eruption of*
805 *Augustine Volcano, Alaska: Professional Paper 1769*, chapter 10, pages 219–
806 267. US Geological Survey, Menlo Park, CA, 2010.
- 807 D. Venezky and C. Newhall. WOVOdat design document: the schema, table
808 descriptions, and create table statements for the database of worldwide volcanic
809 unrest (WOVOdat Version 1.0). *Geological Survey Open File Report 2007-*
810 *1117*, page 184, 2007.
- 811 G. Wadge and M. C. Isaacs. Mapping the volcanic hazards from the
812 Soufrière Hills Volcano, Montserrat, West Indies, using an image proces-
813 sor. *Journal of the Geological Society, London*, 145(4):541–551, 1988. doi:
814 10.1144/gsjgs.145.4.0541.
- 815 S. F. Watt, D. M. Pyle, and T. A. Mather. Evidence of mid- to late-Holocene
816 explosive rhyolitic eruptions from Chaitén Volcano, Chile. *Andean Geology*,
817 40(2):216–226, 2013. ISSN 0718-7106. doi: 10.5027/andgeoV40n2-a02.
- 818 P. L. Whelley, C. G. Newhall, and K. E. Bradley. The frequency of explosive

819 volcanic eruptions in Southeast Asia. *Bulletin of Volcanology*, 77(1):1, 2015.

820 doi: 10.1007/s00445-014-0893-8.

821 C. Widiwijayanti, B. Voight, D. Hidayat, and S. P. Schilling. Objective rapid

822 delineation of areas at risk from block-and-ash pyroclastic flows and surges.

823 *Bulletin of Volcanology*, 71(6):687–703, 2008. doi: 10.1007/s00445-008-0254-

824 6.

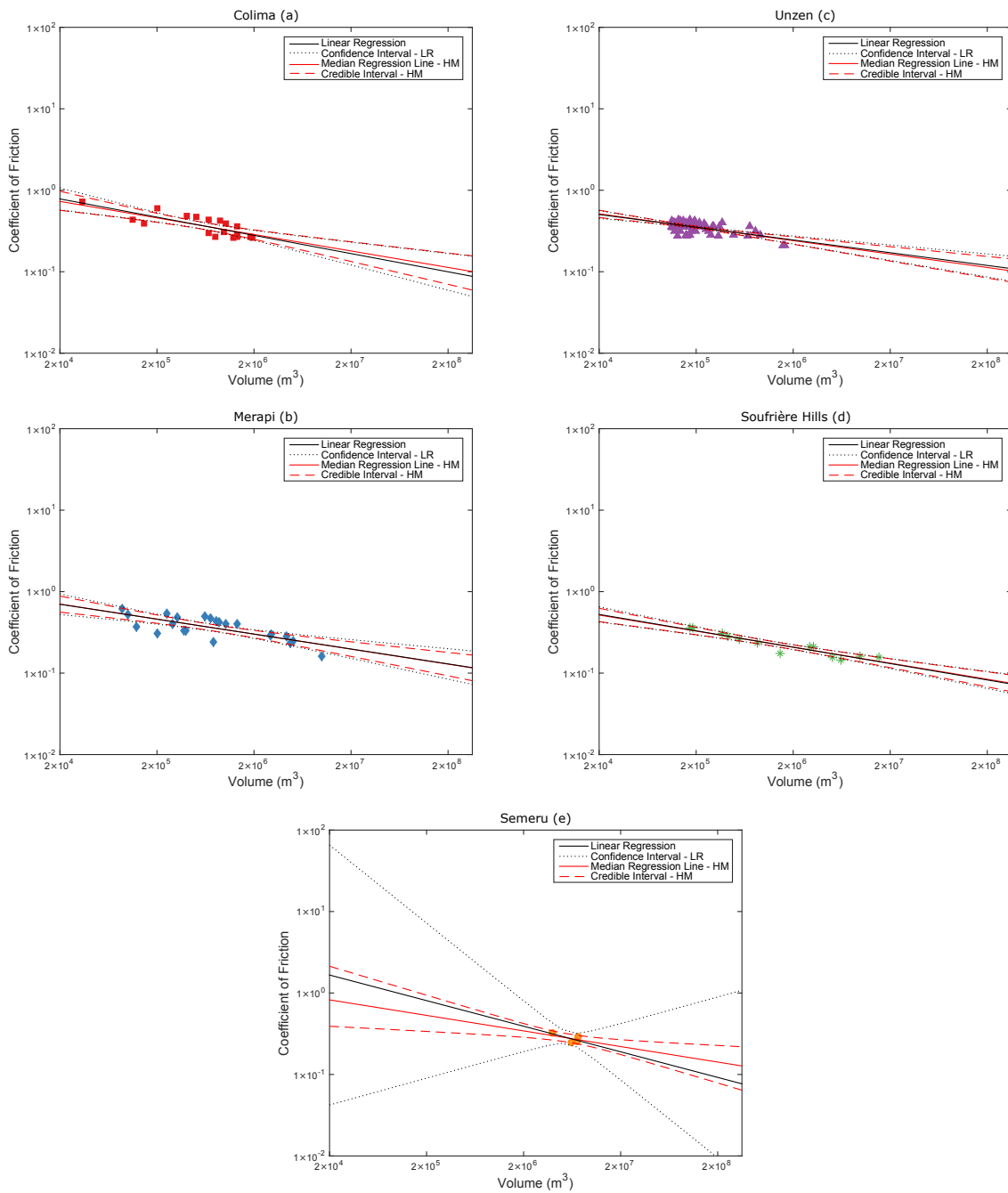


Figure 3: Comparison of the 95% confidence intervals (black dotted line) on the regression line for each individual volcano (black solid lines) and credible intervals (red dotted line) obtained from the hierarchical model (red solid line) as applied to the coefficient of friction vs volume relationship. PDCs in a & b were considered unchanneled; and c & d were considered channeled in this analysis. PDCs from Semeru (e) were also considered channeled, but with only four data points.

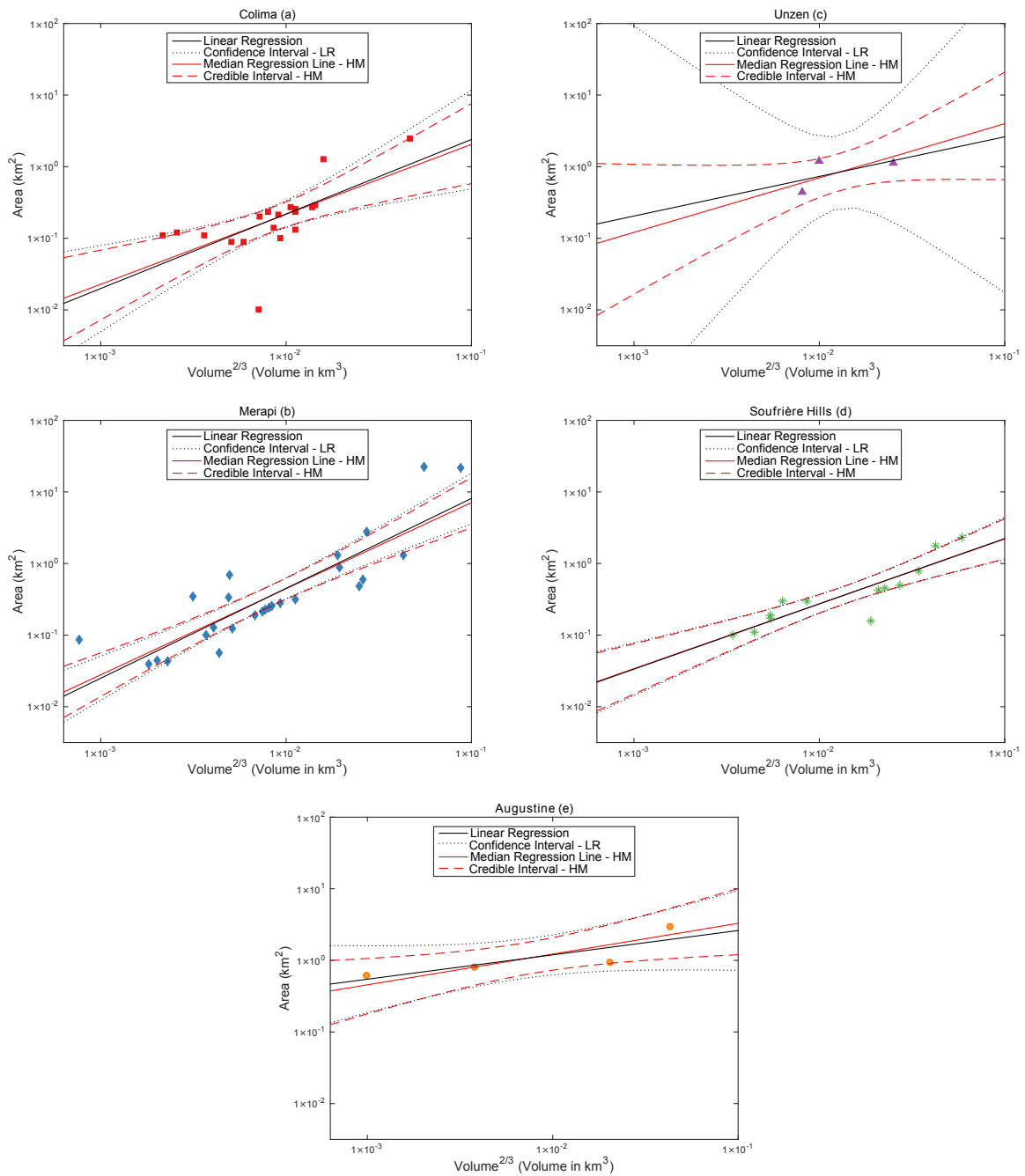


Figure 4: Comparison of the 95% confidence intervals (black dotted line) on the regression line for each individual volcano (black solid lines) and credible intervals (red dotted line) obtained from the hierarchical model (red solid line) as applied to the A_{P4} vs. $V^{2/3}$. PDCs in a & b were considered unchanneled; and c & d were considered channeled in this analysis. Augustine (e) produced unchanneled flows, but which travelled over surfaces of snow and ice.

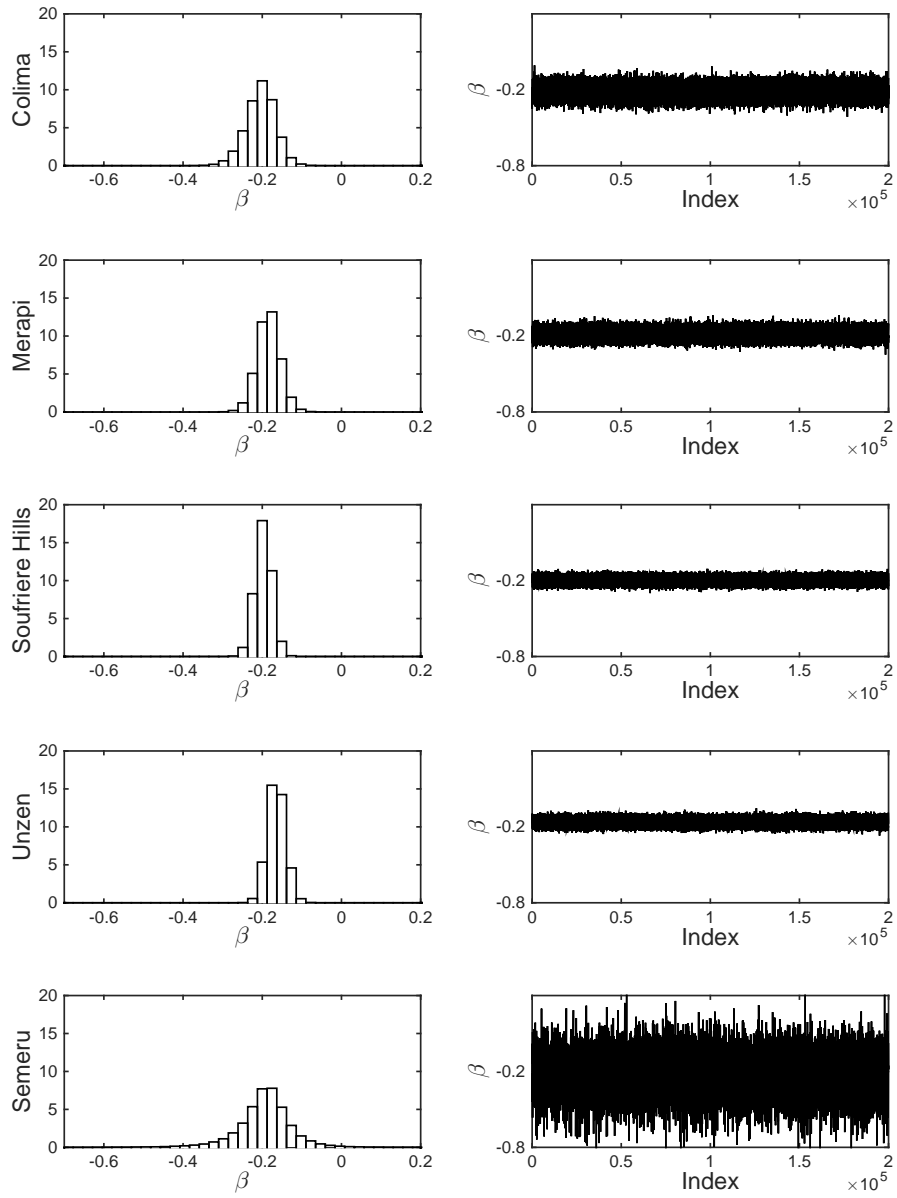


Figure 5: Left: Normalized histograms of sampled slopes for the frictional model for each of the five volcanoes considered. Right: corresponding trace plots from MCMC samples.

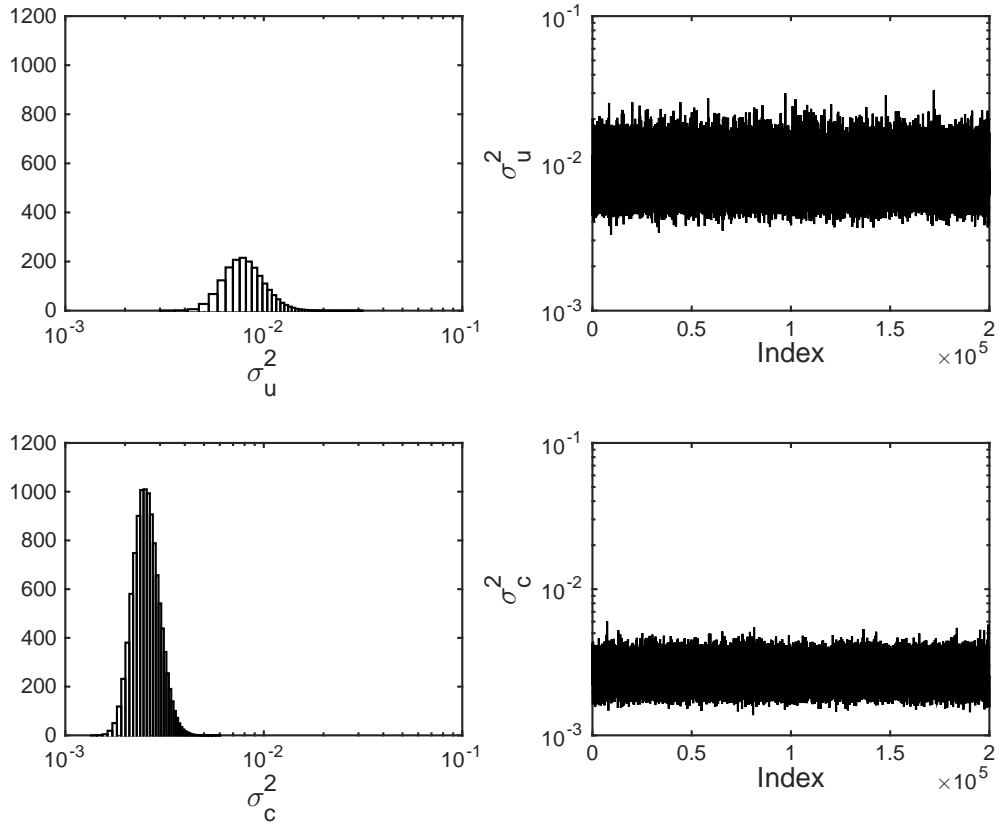


Figure 6: Left: Normalized histograms of the inferential variances, σ_u^2 (unchanneled, top) and σ_c^2 (channelized, bottom), for linear regression model applied to the frictional relationship, plotted on a log scale. Right: corresponding trace plots from MCMC samples.